BENG 221

Hyperthermia Cancer Therapy by Magnetic Nanoparticles

A Mathematical Model of Utilizing Heat Generated from an Alternating Magnetic Field to Kill Cancerous Cells

Jenny Wu
Xuanyi Ma
Yuchen Wang

November 15, 2013

Table of Contents

1. Background and Introduction

Cancer is the general term describing a cluster of cells undergoing uncontrolled growth in the body, also known as a tumor. Benign tumors are simply physical obstructions that may hinder the functionality of the organ, but malignant tumorscan invade surrounding tissues or spread to create a variety of cancerous growths in other parts of the body. The mechanism behind how tumors appear or how cells suddenly become unregulated is poorly understood, but due to the volatile nature of tumors becoming malignant and spreading throughout the body, the field of oncology, especially the study of killing cancerous cells is highly investigated. One method of destroying tumors is magnetic hyperthermia.

1.2 Cancer Treatment by Magnetic Hyperthermia

Tumorous cells die at elevated temperatures, in particular in the range of 42-46°C and since local hyperthermia does not require surgery to administer,the therapy is a very efficient and non-invasive approach for treating cancer. The therapy is so effective that local hyperthermia is used as a supplementary treatment to radiotherapy and chemotherapy.Hyperthermia can be rendered by several different heat sources such as external water baths, radiation applicators, or inserted probes. Unfortunately, these heat sources do not provide enough control or precision of how or how much heatis applied to the target area.

The discovery of generating a localized heat field by exposing magnetic particles to a magnetic alternating current field opened the doors to magnetic hyperthermia [1, 2].The study of different energy dissipation and effects of electromagnetic fields on different particles has shown the superiority of this therapy in providing site-specific heating that minimizes damage to the surrounding tissues [3]. The treatment begins with the injection of magnetic nanoparticles, specifically Fe_3O_4,that are about 10nm in radius and coated with cancer-specific biomolecules, into the blood stream near the tumor where the nanoparticles attach and accumulate[4, 5]. Once adhered to cancerous cells, the nanoparticles are subjected to an alternating magnetic field for 15-60 minutes to gain and maintain a temperature in the range of 42-46°C [6].Figure 1 details the process of magnetic hyperthermia.

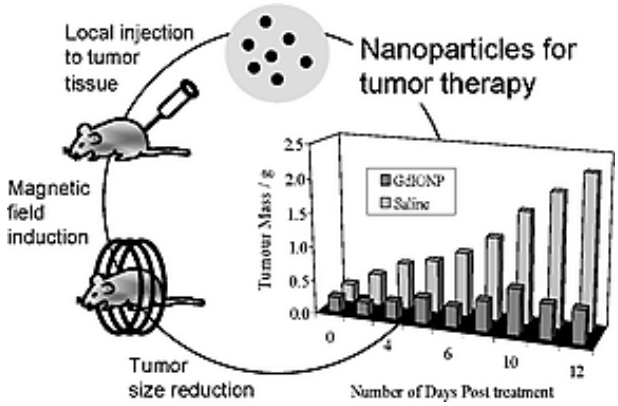

Figure 1: Basic process of magnetic hyperthermia [6].

1.2.1 Hysteresis Loss Described by the Neel and Brownian Relaxation

Hysteresis loss describes the phenomenon of heat generation that results from magnetic particles reacting to an alternating magnetic field [1, 2].When ferromagnetic materials are subjected to a magnetic field, the particles will align themselves according to the magnetic field. In the case of the

alternating magnetic field, the particles are constantly realigning themselves to match the changing magnetic field and after realignment, the energy used for the alignment is released during the relaxation of when the magnetic moment returns to the equilibrium orientation. The released energy dissipates as heat where the Neel and Brownian Relaxation models describe the non-rotational and rotational motion of particles during their relaxation respectively [2]. The overall behavior and heat generation phenomenon is described as hysteresis loss as depicted visually in Figure 2.

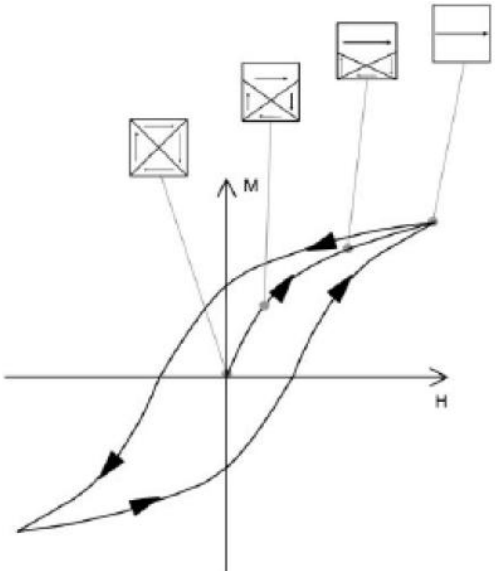

Figure 2: Hysteresis cycle of a magnetic material where H is the magnetic field amplitude and M is the magnetization of the material. The arrows indicate the direction of the magnetization [3].

1.2.2 Characterization of Nanoparticles by Specific Loss Power (SLP)/Power Density

Nanoparticles made of different materials exhibit different hysteresis loss profiles and the best approach in implementing magnetic hyperthermia would be to determine what material type could generate the best temperature range with the least amount of nanoparticles. The parameter, specific loss power (SLP), measured by power per mass unit, best determines the amount of heat, related to power, that the particles can generate and is dependent the size, distribution, shape, and chemical composition of the particles [2]. For our model, we converted the SLP into power density measured by power per volume unit that better describes the driving force of the magnetic hyperthermia.

2. Modeling Strategy

Although magnetic hyperthermia is an effective cancer therapy, limitations restrict the treatment to tumors growing in specific tissues in the body. Limitations include blood perfusion that leads to large amount of blood removing heat from the tissue as they circulate the body and the size the nanoparticles restricting them from traveling into the smaller capillaries inside the tumor growth. Such restrictions prevent magnetic hyperthermia from treating brain tumors where the blood-brain barrier does not allow injected nanoparticles to accumulate effectively on the tumorous growths.The high blood perfusion nature of the lungs also results in rapid heat dissipation before the nanoparticles can even reach the elevated temperature range to kill the cancerous cells. The low heat diffusivity and general

difficulty in pinpointing tumors in bone also makes magnetic hyperthermia another poor treatment approach.

2.1 Liver Tumor

However, in liver tissue, tumorous liver tissue actually exhibit lower blood perfusion than in healthy liver tissue thus resulting in a semi-protection for the healthy tissue during local hyperthermia treatment [7]. The decrease in blood perfusion in the tumor leads us to define the model of the liver tumor such that blood circulation decreases from the peripheral to the center of the tumor. The decrease in blood circulation also means a lower concentration of the nanoparticles will be inside the tumor, which leads to a lower heat generation by the particles the closer our model is to the center of the tumor.

3. Mathematical Model

3.1 Assumptions

In our mathematical model, we assume the tumor is spherical in shape and that the concentration of particles from the peripheral to the center of the tumor is decreasing in a linear relationship. The linear correlation of the decreasing particle concentration also applies to the power density. At initial conditions before the start of the treatment, we also assume that the tumor to have the same temperature as the healthy tissue, which is at body temperature ($T_0 = 37°C$). We also assume that at the boundary of the tumor and healthy tissue ($r = R$), the body maintains a constant homeostasis environment of the body temperature. In order to provide a solution for our model, we must also assume that the temperature of the tumor is and will always be finite.

3.2 Basic Model

Before we simulate the real heat diffusion process, we need to determine the heat conductance of the specific tumor; hence, we can use our first model to decide the constant. Based on the assumption in which we assume a linear power density, the spherical shape of the tumor, and the boundary is symmetrical under spherical coordinates, we can write the diffusion equation into the form:

$$c_1\rho_1\frac{\partial T}{\partial t} = k_1\frac{1}{r^2}\frac{\partial}{\partial r}(r^2\frac{\partial T}{\partial r}) + wr$$

In the equation, c_1 is the specific heat of the tumor, ρ_1 is the density of the tumor, and k_1 is the heat conductance. The former two variables are easily attainable throughexperimental analysis as opposed to the heat conductance where we will need to determine a correlation between the value of heat conductance with specific heat and density.Theinitial and boundary conditions are shown below:

$$T(r,0) = T_0$$
$$T(0,t)\ finite$$
$$T(r,t) = T_0$$

Tosimplify the equation, we transform T into a new variable by the following transform:

$$\Phi(r,t) = r(T(r,t) - T_0)$$

After applying the transform into the original equation, we obtain the followingequation:

$$\frac{1}{D_1}\frac{\partial \Phi}{\partial t} = \frac{\partial^2 \Phi}{\partial r^2} + \frac{w}{k_1} r^2$$

Having transformed the original equation into a new variable, we also transform the conditionsinto terms of Φ . Note that we can only transform the boundary condition at $r = 0$ if we had assumed that the temperature of the tumor is finite:

$$\Phi(0,t) = \lim_{t \to 0} r(T(r,t) - T_0) = 0 \text{ (forwhen } T(0,t) \text{ is finite)}$$
$$\Phi(R,t) = R(T(R,t) - T_0) = 0$$
$$\Phi(r,0) = r(T(r,0) - T_0) = 0$$

The homogeneous boundary conditions and the source term in the equationallow us to break the solution into the steady and the homogenous term. When the solution reaches the steady state, the equation becomes:

$$\frac{\partial^2 \Phi_s}{\partial r^2} + \frac{w}{k_1} r^2 = 0$$

With the conditions:

$$\Phi_s(0,t) = 0$$
$$\Phi_s(R,t) = 0$$
$$\Phi_s(r,0) = 0$$

From those conditions, we can arrive at the steady state solution:

$$\Phi_s(r,t) = \frac{w}{12k_1} r(R^3 - r^3)$$

We then solve for the homogeneous solution with the remaining portion of theequationwith the same conditions as follows:

$$\frac{1}{D_1}\frac{\partial \Phi_h}{\partial t} = \frac{\partial^2 \Phi_h}{\partial r^2}$$
$$with$$
$$\Phi_h(0,t) = 0$$
$$\Phi_h(R,t) = 0$$
$$\Phi_h(r,0) = -\frac{w}{12k_1} r(R^3 - r^3)$$

Using the separation of variables again, we arrive at the solution:

$$\Phi_h = \sum_{n=1}^{\infty} \frac{2wR^4(-1)^n}{(n\pi)^3}[1+\frac{2}{(n\pi)^2}((-1)^n-1)]\sin(\frac{n\pi}{R}r)e^{-D_1(\frac{n\pi}{R})^2 r}$$

Combining the steady-state solution with the homogenoussolution and using the reverse transform, we can obtain the final solution for T:

$$T(r,t) = T_0 + \frac{w}{12k_1}(R^3 - r^3) + \sum_{n=1}^{\infty} \frac{2wR^3(-1)^n}{(n\pi)^2}[1+\frac{2}{(n\pi)^2}((-1)^n-1)]\sin c(\frac{n\pi}{R}r)e^{-D_1(\frac{n\pi}{R})^2 r}$$

$$\text{In which } \sin c(x) = \frac{\sin(x)}{x}$$

As time continues, the temperature across the whole tumor will almost reach steady state at which point, we can measure the final temperatureof the tumor (denoted by T_s). With that measurement and the measurement of the original temperature of the tumor at T_0, we can determine the heat conductance of specific tumor by using the relationship deduced from the $T(r,t)$ solution below, which can then be used to simulate the realistic heat diffusion from the tumor to its surrounding tissue in a more advanced model:

$$T_s = T_0 + \frac{w}{12k_1}R^3$$

3.2.1 Results

Using the following parameters taken from various literature sources, we can test our basic model with the MATLAB code documented in the Appendix.

Parameter	Constant	Value
Liver Tissue Heat Conductance	k_1	0.5122 $\frac{W}{m \cdot K}$
Liver Density	ρ_1	1.0492 $\frac{g}{mL}$
Tumorous Liver Tissue Specific Heat	c_1	3.758 $\frac{kJ}{kg \cdot K}$
Radius of Liver Tumor	R	2.50 cm
Power of Nanoparticles	P	200 W

Table 1: Liver tissue and nanoparticle parameters taken from various literature sources [8, 9, 10, 11].

Running the code returns the following plots in Figure 3 and 4. As expected, the temperature reaches its peakof about 42.5°C at the center of the tumor($r = 0$) whereas the temperature drops off to body temperature at the interface between the tumor and healthy tissue ($r = R$).

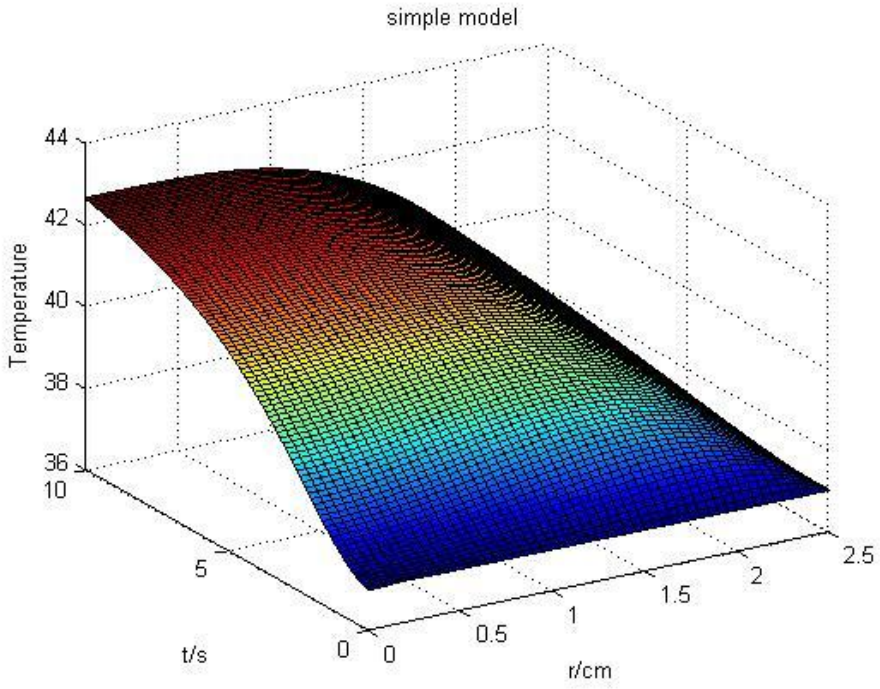

Figure 3: Surface plot depicting the temperature in terms of time and distance from the center of the tumor.

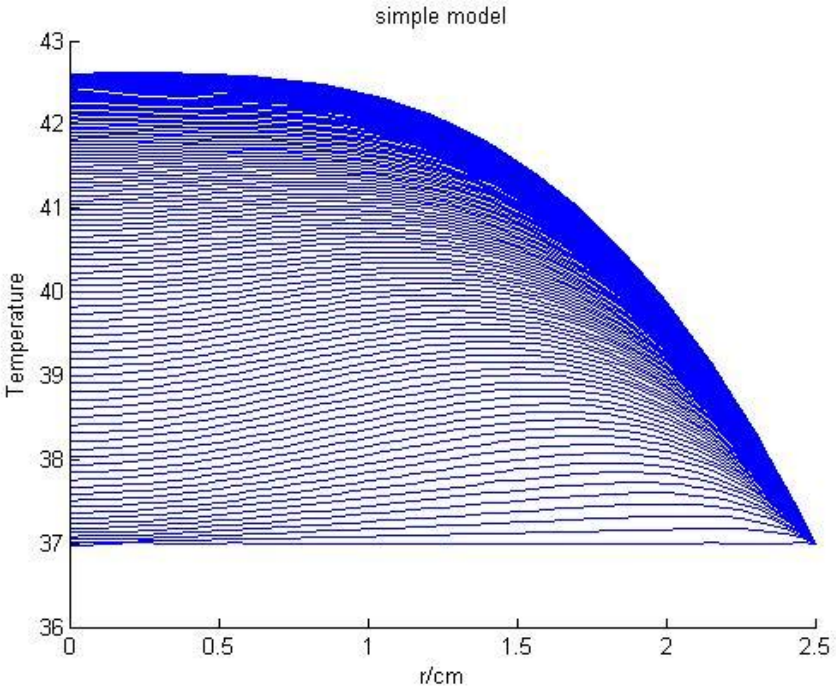

Figure 4: Plot of the temperature over the radius of the tumor. Each individual line is a specific time point.

3.3 Advanced Model

In the second model, we attempt to simulate the realistic heat diffusion from the tumor to its surrounding tissue. In the basic model, we assumed that the temperature inside and outside the tumor are independent of each other, but in reality, the two temperatures influence each other at the boundary interface.In addition, due to the heat induced by the magnetism in the tumor, the twodiffusion equations are differentfrom each other as shown:

$$c_1\rho_1\frac{\partial T_1}{\partial t}=\frac{k_1}{r^2}\frac{\partial}{\partial r}\left(r^2\frac{\partial T_1}{\partial r}\right)+P$$
$$c_2\rho_2\frac{\partial T_2}{\partial t}=\frac{k_2}{r^2}\frac{\partial}{\partial r}\left(r^2\frac{\partial T_2}{\partial r}\right)$$

Based on the assumption that the temperature and flux at the boundary are fine and continuous, the following conditions are true:

$$T_1(R,t)=T_2(R,t)$$
$$k_1\frac{\partial T_1(R,t)}{\partial r}=k_2\frac{\partial T_2(R,t)}{\partial r}$$
$$T_1(0,t)\ finite$$
$$T_1(r,0)=T_0$$
$$T_2(r,0)=T_0$$

In which T_1 and T_2 denotes the temperature inside and outside the tumor separately.

Due to the complexity of solving of the equation analytically, we chose to use the numerical method to solve the problem. Then we will transform the continuous equation into the difference equation using the Euler's method.

Since the flux is one-sided for $r=0$, the numerical approximation for the boundary condition in the center is:

$$c_1\rho_1\frac{\partial T(0,t)}{\partial t}\Delta V=c_1\rho_1\frac{\partial T(0,t)}{\partial t}Adr=-k_1\frac{\partial T(0,t)}{\partial r}A+PAdr$$
$$T_1(0,t+\Delta t)=T_1(0,t)+\frac{k_1\Delta t}{c_1\rho_1\Delta r^2}(T_1(\Delta r,t-\Delta t)-T_1(0,t-\Delta t))+\frac{P\Delta t}{c_1\rho_1}$$

$$T_1(r,t+\Delta t)=T_1(r,t)+\frac{k_1\Delta t}{c_1\rho_1\Delta r^2}[T_1(r+\Delta r,t-\Delta t)-T_1(r,t-\Delta t)-$$
$$(1-(\frac{\Delta r}{r})^2)(T_1(r,t-\Delta t)-T_1(r-\Delta r,t-\Delta t))]+\frac{P\Delta t}{c_1\rho_1}(0<r<R)$$

Using the same process, the second equation can be deducedfrom the boundary condition at the tumor-healthy tissue edge and results in the following to equations:

$$T_2(r,t+\Delta t) = T_2(r,t) + \frac{k_2 \Delta t}{c_2 \rho_2 \Delta r^2}[T_2(r+\Delta r, t-\Delta t) - T_2(r,t-\Delta t) -$$

$$(1-(\frac{\Delta r}{r})^2)(T_2(r,t-\Delta t) - T_2(r-\Delta r, t-\Delta t))](r > R)$$

$$T_1(R,t) = T_2(R,t) = \frac{k_1 T_1(R-\Delta r,t) + k_2 T_2(R+\Delta r,t)}{k_1 + k_2}(r = R)$$

3.3.1 Results

Using the following parameters taken from various literature sources, we can test our advanced model with the MATLAB code documented in the Appendix.

Parameter	Constant	Value
Liver Tissue Heat Conductance	$k_1 = k_2$	0.5122 $\frac{W}{m \cdot K}$
Liver Density	$\rho_1 = \rho_2$	1.0492 $\frac{g}{mL}$
Healthy Liver Tissue Specific Heat	c_2	3.617 $\frac{KJ}{kg \cdot K}$
Tumorous Liver Tissue Specific Heat	c_1	3.758 $\frac{KJ}{kg \cdot K}$
Radius of Liver Tumor	R	2.50 cm
Power of Nanoparticles	P	6.5W

Table 2: Liver tissue and nanoparticle parameters taken from various literature sources [8, 9, 10, 11].

Running the code generates the following plots in Figure 5 and 6. At the boundary, $r = R$,the temperature is higher than predicted in the basic model because the surrounding tissues' temperature is also raised by the hyperthermia treatment in the tumor, which is what occurs in reality. In addition, the temperature peaks at a higher value due to the influence of the hyperthermia treatment affecting the homeostasis element of the healthy tissue at the boundary conditions.

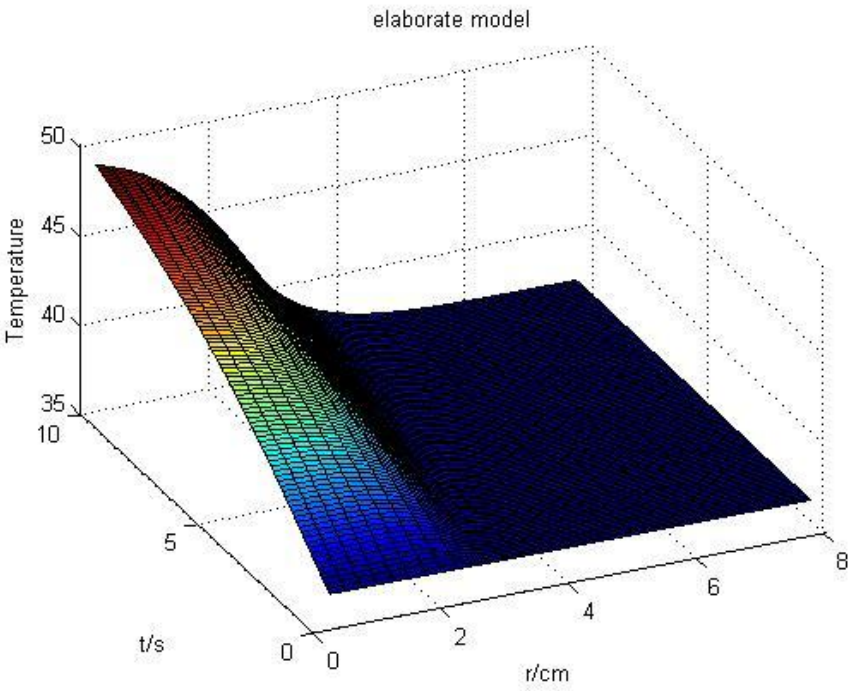

Figure 5: Surface plot depicting the temperature in terms of time and distance from the center of the tumor according to the advanced model.

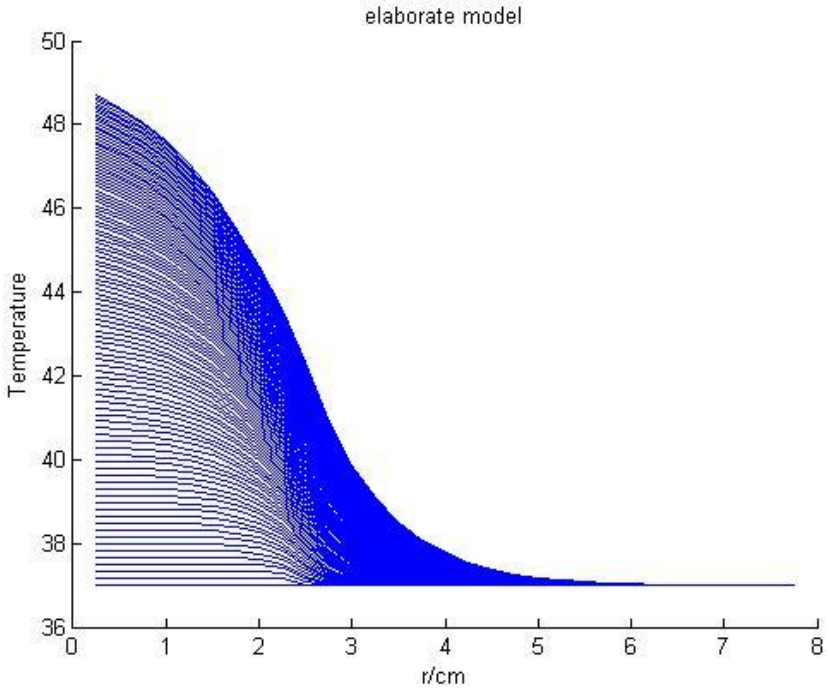

Figure 6: Plot of the temperature over the radius of the tumor according to the advanced model. Each individual line is a specific time point.

4. Discussion

We modeled the temperature changes of the cancer treatment, magnetic hyperthermia, by using both a basic and advanced model. The heat diffusivity of magnetic hyperthermia in a tumor is essentially the partial differential equation (PDE) of heat diffusivity with a heat source in spherical coordinates. The heat source is dependent on the power density that is in turn dependent on the type and amount of nanoparticles used for the treatment. Although the specific heat and density of the tissue of interest can be measured experimentally, the heat conductance is harder to determine. However, solving the basic model at steady-state allows us to determine the heat conductance of the specific tumor that we want to kill. With that specific heat conductance, we can use the value in the more advance model for meaningful results. As we did not have a real liver tumor to measure, we resorted to literature sources for the needed parameters. Our basic model depicted a steady-state at roughly t=10 seconds and a peak of 42.5°C in the center of the tumor at r=0.

In the advanced model, we created a more accurate interface at the boundary conditions by defining the temperature of the tumor's exterior as a function that can be affected by the tumor's interior temperature during the hyperthermia treatment. Instead of a sudden cutoff to body temperature at the boundary, the advanced model displayed a temperature curve that describes how the tumor's interior can also heat up the immediate region of tissue at the tumor's exterior. Without the assumption of a constant homeostasis of body temperature at the boundary results in a higher peak temperature of 48°C, but still the model can still reachsteady state within 10 seconds. To make this a safer treatment, less nanoparticles or nanoparticles of different material will need to be utilized to reach a lower peak temperatureand will not cause the external healthy tissue to heat up so high.

In conclusion, magnetic hyperthermia is a very effective method for cancer treatment with a highly controllable modus operandi dependent on the material and amount of nanoparticles. The additional possibility of coating the nanoparticles in tumor-specific biomolecules adds further precision to the method that promotes safety.

4.1 Future Investigation

For simplicity, we had assumed the tumor is spherical in shape, but physiologically, tumors rarely grow into perfect spheres. To make our model more accurate, we would need to redefine the shape of our tumor to that of a more irregular globular shape. In addition, the initial condition may not be as global as we assumed where the entire environment is at body temperature. We had also assumed the same heat conductance and density for both healthy and tumorous liver tissue when they are two different tissue types. In particular, tumorous tissue is rarely uniform and the parameters that govern the diffusivity across the tissue can vary in the different dimensions depending on what cancerous cells are growing. We had also assume that the distribution of the nanoparticles to be decreasing in a linear fashion, which meant that the power density would also be linear. However, given the tumultuous environment inside the tumor, the probability of the nanoparticles distributing linearly perfectly through the tumor is unlikely. Instead, the power density of the nanoparticles may be higher in one quadrant while maybe negligible in another. We had attempted to create a more realistic model in our advanced model by including an expression that describes the influence of the internal and external temperatures on each other. However, we did not include other factors such as the consumption rate or effects of blood perfusion in the healthy tissue. For future analysis, the inclusion of a more accurate tumor shape, different initial conditions in different dimensions, varying diffusivity constants in different dimensions, the real distribution of nanoparticles, and additional effects on the tumor-healthy cells interface can provide a more accurate model of magnetic hyperthermia.

Appendix

```
closeall;
clearall;
clc;
%%%%%%%%%%%%%%%%%%%%%%%%%%%%%%%%%%%%%%%%%%%%%%%%%%
%% BENG221   Project                          %%
%%%%%%%%%%%%%%%%%%%%%%%%%%%%%%%%%%%%%%%%%%%%%%%%%%
%% Part One
%% Constant
T0 = 37;
R  = 2.5;
P  = 200;
w  = P/(4/3*pi*R^3);
k  = 0.642;
D  = 0.642/3.72;
T_range = 10;
dt = 0.1;
t = 0:dt:T_range;
dr = 0.05;
r = 0:dr:R;
N_term = 15;
n = 1:N_term;

%% Analytical result

T = T0 + w/k/12.*(R^3 - r'.^3)*ones(1,length(t)) + sinc(r'./R *
n)*diag(2*w*R^3/pi^2/k.*(-1).^n./n.^2.*(1+2/pi^2.*((-1).^n - 1)./n.^2))...
    * exp(-D*pi^2/R^2.*n'.^2 * t);

figure,surf(t,r,T);
xlabel('t/s');
ylabel('r/cm');
zlabel('Temperature');
title('simple model');

figure,
holdon;
forcnt = 1:length(t);
plot(r,T(:,cnt));
end
holdoff;
xlabel('r/cm');
ylabel('Temperature');
title('simple model')
% xv = -4:0.01:4;
%yv = -4:0.01:4;
% t  = 1:1:15;
%
% TT = @(r,t) T0 + w/k/12.*(R^3 - r^3)+ sinc(r'./R *
n)*diag(2*w*R^3/pi^2/k.*(-1).^n./n.^2.*(1+2/pi^2.*((-1).^n - 1)./n.^2))...
%     * exp(-D*pi^2/R^2.*n'.^2 * t);
% for t_index = 1:length(t)
%
% for x_index = 1:length(xv)
%     for y_index = 1:length(yv)
```

```
%
%     if sqrt(xv(x_index).^2 + yv(y_index).^2) > R
%      T(y_index,x_index,t_index) = T0;
%     else
%     T(y_index,x_index,t_index) = TT(sqrt(xv(x_index).^2 +
yv(y_index).^2),t(t_index));
%     end
%     end
% end
% end
% [X,Y] = meshgrid(xv,yv);
% figure('Renderer','zbuffer')
% F(15) = struct('cdata',[],'colormap',[]);
%
% for cnt = 1:15
% mesh(X,Y,T(:,:,cnt));
% axis([-4 4 -4 4 36 43])
% F(cnt) = getframe;
% end
% movie(F,20)


%% Part Two
%% constant
cp_1 = 1.0492*3.758;
cp_2 = 1*3.615;
k_1  = 0.778;
k_2  = 0.642;
P    = 6.5%12.3;
q_k  = k_2/k_1;
q    = cp_2/cp_1;
R    = 2.5 %0.7;
dr   = R/10;
D    = 3*R;
T0   = 37;
dt   = 0.1;
T_range  = 10;
t        = 0:dt:T_range;
rv_1 = dr:dr:R;
rv_2 = R+dr:dr:D+dr*length(t);
rv   = [rv_1 rv_2];
T    = T0.*ones(length(rv),length(t));
%% function
%
% s   = @(z) (q_k - 1).*sin(z) +z .* cos(z);
% f   = @(z,r,t) z.^(-2).*exp(-k_1/cp_1.*t.*z.^2./R.^2).*((z.*cos(z) -
sin(z))./(s(z).^2 + q_k*q.*(z.*sin(z)).^2));
% k   = @(z,r) sqrt(q_k*q).*z.*(r./R - 1);
% g_1 = @(z,r) sin(r.* z ./R);
% g_2 = @(z,r) s(z).* sin(k(z,r)) + sqrt(q_k*q).*z.* sin(z).* cos(k(z,r));
%
% %% integrate
% delta_T   = zeros(length(t),length(rv));
% for t_index = 1:length(t)
%     z = [0.01:0.01:1e5];
%     for r_index_1 = 1:length(rv_1);
```

```
%         intv =
trapz(z,f(z,rv_1(r_index_1),t(t_index)).*g_1(z,rv_1(r_index_1)));
%         delta_T(t_index,r_index_1) = P*R^2/3/k_2 * (1 + q_k/2*(1 -
rv_1(r_index_1)^2)) + 6/pi*q_k^1.5*q^0.5 * R/rv_1(r_index_1)* intv;
%     end
%     for  r_index_2 = 1:length(rv_2);
%         intv =
trapz(z,f(z,rv_2(r_index_2),t(t_index)).*g_1(z,rv_2(r_index_2))./z);
%         delta_T(t_index,length(rv_1)+r_index_2) =
P*R^3/3/k_2/rv_2(r_index_2).*(1+6/pi*q_k * intv);
%     end
% end
% T = T0 + delta_T';
% figure,surf(t,rv,T);
```

```
cnt  = 1;
fort_index = 2:length(t);
T(1,t_index) = T(1,t_index - 1) + k_1/cp_1*dt/dr^2*(T(2,t_index - 1)-
T(1,t_index - 1)) + P/cp_1*dt;
forr_index = 2:(length(rv_1)-1);
   T(r_index,t_index) = T(r_index,t_index - 1) +
k_1/cp_1*dt/dr^2*(T(r_index+1,t_index - 1)-T(r_index,t_index - 1)-(1-
2*dr/rv(r_index))*(T(r_index,t_index - 1)-T(r_index-1,t_index - 1))) +
P/cp_1*dt;
end
   T(length(rv_1),t_index) = (k_1*T(length(rv_1)-1,t_index-1) +
k_2*T(length(rv_1)+1,t_index-1))./(k_1+k_2);
forr_index = (1+length(rv_1)):(length(rv)-cnt);
   T(r_index,t_index) = T(r_index,t_index - 1) +
k_2/cp_2*dt/dr^2*(T(r_index+1,t_index - 1)-T(r_index,t_index - 1)-(1-
2*dr/rv(r_index))*(T(r_index,t_index - 1)-T(r_index-1,t_index - 1)));
end
end

figure,surf(rv(1:(length(rv)-100)),t,T(1:(length(rv)-100),:)');
xlabel('r/cm');
ylabel('t/s');
zlabel('Temperature');
title('elaborate model');
figure
holdon
forcnt = 1:length(t);
    plot(rv(1:(length(rv)-100)),T(1:(length(rv)-100),cnt));
end
holdoff
xlabel('r/cm');
ylabel('Temperature');
title('elaborate model');
```

References

[1] Andra W, d' Ambly CG, Hergt R. Temperature distribution as function of time around a small spherical heat source of local magnetic hyperthermia. Journal of Magnetism and Magnetic Materials. 1999. 194: 197-203.
[2] Hergt R, Dutz S, Muller R, et al. Magnetic particle hyperthermia: nanoparticle magnetism and materials development for cancer therapy.Journal of Physics: Condensed Matter. 2006. 18: S2919-S2934.
[3] Mornet S, Vasseur S, Crasset F, et al. Magnetic nanoparticle design for medical diagnosis and therapy. J. Mater. Chem. 2004.14: 2161-2175.
[4] Montet X, Funovics M, Montet-Abou K, et al. Multivalent effects of RGD peptides obtained by nanoparticle display. J Med Chem. 2006.49(20): 6087-6093.
[5] Zhao, DL, Zeng XW, Xia QS, et al. Preparation and coercivity and saturation magnetization dependence of inductive heating property of Fe_3O_4 nanoparticles in an alternating current magnetic field for localized hyperthermia. Journal of Alloys and Compounds.2009. 469(1-2): 215-218.
[6] Shido Y, Nishida Y, Suzuki Y, et al. Targeted hyperthermia using magnetite cationic liposomes and an alternating magnetic field in a mouse osteosarcoma model. J Bone Joint Surg Br. 2010. 94(4): 580-585.
[7] Tsafnat N, Tsafnat G, Lambert TD, et al. Modeling heating of liver tumors with heterogeneous magnetic microspheres disposition. Physics in Medicine and Biology. 2005. 50: 2937-2953.
[8] Valvano JW, Cochran JR, Diller KR. Thermal conductivity and diffusivity of biomaterials measured with self-heated thermistors. *International Journal of Thermophysics*. 1985. 6(3): 301-11.
[9] Howells CC, Stinauer MA, Diot Q, et. al. Normal Liver Tissue Density Dose Response in Patients Treated With Stereotactic Body Radiation Therapy for Liver Metastases. International Journal of Radiation Oncology*Biology*Physics. 2012. 84(3): e441–e446.
[10] Giering K, Lamprecht I, Minet O, et. al. Determination of the specific heat capacity of healthy and tumorous human tissue. ThermochimicaActa. 1995. 251(1): 199-205
[11] Andra W, d' Ambly CG, Hergt R. Temperature distribution as function of time around a small spherical heat source of local magnetic hyperthermia. Journal of Magnetism and Magnetic Materials. 1999. 194: 197-203.